An investigation of plasma sprayed nickel-based and pure aluminum coatings on austenitic stainless steel AISI 304

An investigation of plasma sprayed nickel-based and pure aluminum coatings on austenitic stainless steel AISI 304

K. Hamed[1], N. El-Mahallawy[2] and M.O.A. Mokhtar[3]

[1] M.Sc. Student, Design and Production Engineering Department, Faculty of Engineering, Ain Shams University, Egypt
[2] Professor Dr., Design and Production Engineering Department, Faculty of Engineering, Ain Shams University, Egypt
[3] Professor Dr., Department of Mechanical Design and Production, Faculty of Engineering, Cairo University, Egypt

E-mail: 13084@eng.asu.edu.eg

Abstract Atmospheric Plasma Spray (APS) is one of the most leading industrial techniques for protective coating, by improving the performance of parts in the thermal barrier, and wear resistance. Ni-Al alloys are very effective players in the field of design of protective coatings. Accordingly, mixed Al, Ni/Al, and Ni5Al powders were applied on 304stainless steel substrate to develop plasma sprayed coatings. The effect of different compositions on microstructure, microhardness, and porosity was measured. The microstructures of the as-deposited films were characterized utilizing X-ray diffraction (XRD), scanning electron microscopy (SEM), and microhardness measurements. The results showed the formation of two intermetallic compounds, namely: NiAl and Ni3Al. The existence of NiAl is inevitable in all samples, despite the amount of Ni-based alloys in mixtures, or even the atomic percentage of nickel, where the appearance of Ni3Al depends only on increasing the amount of the Ni-based alloy to 50 % percent in mixtures. As regards the steel substrate, the microhardness of the interdiffusion zone of the substrate has been significantly enhanced. Results have shown that the microhardness of the different tested coatings is increased directly with the increment of Ni-based percentage in the coating mixture. The average porosity of the plasma sprayed coatings has proven to be within the normal range.

1. Introduction

Thermal spraying serves a wide range of industrial applications through different coating materials. Metallic, ceramic, and some polymeric materials in the form of powder, ceramic rod, or wire can be used to develop a coating. The diversity in materials and techniques is the main advantage of thermal spraying technology. Besides, the process has the ability of coating production without extremely heating the substrate [1], [2]. Applications of protection have always been a great concern to research society when it comes to mechanical parts that are subjected to structural failures during operation. This can be widely seen in gas turbine systems. Thus, boosting the efficiency can be maintained through the design of a thermal barrier coating (TBC). The TBC structure is based on two layers regardless of the substrate underneath. The layer just above the substrate is the bond coat while the final layer is named the topcoat. One of the most leading industrial techniques for depositing protective coatings is Atmospheric plasma spraying (APS); APS enhances part's performance in wear, corrosion, and can deposit layers as a thermal barrier, which have an impact on parts' life, value, and machinery downtime.

During the spraying process, powders are heated to be molten droplets and then accelerated by the heat source, whereupon the molten droplets impact the substrate and rapidly solidify to form a coating layer. Porosity and cracks are the two critical features that must be tightly controlled. They are formed during the process of solidification of impacting particles. Porosity level depends on the process parameters; speed, spray distance, and particle size [3]–[5]. The porosity of thermal spray coatings is usually between 5 – 15% by volume. However, it could be controlled in APS to reach approximately 7%. The major disadvantage of plasma spraying technology is the line-of-sight. Accordingly, the substrate surface must be visible to the area of motion of the APS torch [6]–[9].

Austenitic stainless steel (304) has been chosen as a substrate due to its good corrosion resistance and excellent creep rupture strength; it has been extensively utilized in the manufacturing of many components of conventional power plants [10]–[13]. However, its low corrosion resistance in high-temperature environments makes it essential to develop a protective layer.

Using Aluminum-based coatings in different industries, e.g., aerospace and automotive is attributable to its high strength-to-weight ratio, high electrical and thermal conductivity, adequate corrosion resistance, and affordable metal. These properties made Aluminum-based coating is an optimum choice for steel protection against corrosion with suitable cost reduction. Despite all these advantages, low hardness could be the main limitation for Aluminum to be widely used [14], [15].

On the other hand, according to Kadir [16], nickel alloys are good candidates for bond coat layers in high-temperature applications due to their high melting temperature, good mechanical properties, and oxidation resistance. Ni-Al-based alloys, in particular, have high oxidation resistance, high hardness, and low density [17], [18]. As stated by many studies, the most common stable intermetallic compounds are NiAl and Ni3Al; their excellent mechanical strength, desirable wear-resistant, and sufficiently high melting temperature (1640 ◌C and 1390 ◌C, respectively), provide sustainable performance at elevated temperature. [19]–[27].

Ni/Al[28] and Ni5Al [3], [15] powders are extensively configured with APS [29]–[31], with adequate processing parameters and appropriate measures that exhibit adequate adherence to the substrate and required thickness [17]. They exothermically react and provide nickel aluminides phases, which is mainly used as an effective bond coat for thermal barrier coating [32]. For instance, a study of Ni5Al coating on three types of superalloys in [33] stated that the coating provided good protection in an aggressive environment, especially for Superfer 800.

Ni3Al [34]–[37] and NiAl [6], [10], [31], [38] are potential intermetallic alloys that have an adequate yield strength that proportionally increases with temperature, low density, and high melting point. Enough Aluminum in their compositions could form, in oxidizing environments, thin films of Alumina (Al2O3), which in turn results in excellent oxidation resistance, compact and protective coating.

In practice, the coating is not affected only by a single service condition, but many conditions appear simultaneously [32], [39]–[41]. The coating must sufficiently resist various types of wear and corrosion. Therefore, it has come to mind to use Ni-Al powders in the Aluminum coating matrix, which in turn, could be a suitable additive to pure Aluminum to enhance coating hardness [42]–[44].

The present work is an investigation on stainless steel coating performance, morphology, and microstructure adopting mixtures of Ni/Al or Ni5Al with pure Aluminum as coating materials prepared by atmospheric plasma spraying technique deposited on a stainless-steel substrate.

2. Experimental procedures

Austenitic Cr-Ni stainless steel (AISI 304) has been selected as a Substrate due to its practical application in cases where high wear and corrosion resistance are of prime importance. Atmospheric Plasma Spray (APS) has been applied for surface coating with preassigned powders. Different samples of powders of Ni/Al or Ni5Al have been mixed with pure Aluminum powder at different percentages. Table 1 shows compositions of powder mixtures of tested samples. To maintain uniformity during the deposition, all the powders were thoroughly mixed via ball milling for 6 hours at 200 rpm.

Table 1 Composition of different sprayed coating powders

Sample	Compositions (wt. %)		
	Ni/Al (80/20)	Ni 5Al (95/5)	Pure Al
1A	10	-	90
3A	30	-	70
5A	50	-	50
1B	-	10	90
3B	-	30	70
5B	-	50	50

The substrate samples were flat-strips 30 x 100 x 2.5 mm in size with 2.5 mm sheet thickness. The first step before coating, surface cleaning, and preparation was precisely held to maintain good coat quality. The surfaces of samples were degreased with TCE (Trichloroethylene C2HCL3) for removing surface impurities, then roughened using a blasting procedure with Corundum 500 and blow pressure 5 bar. This surface preparation procedure helped to activate the surface and offered an increased surface area for full adhesion of the sprayed particles. The main spraying parameters employed are shown in Table 2.

Table 2 APS process parameters

Parameter	Value
Gun	F4 – MB
Gas	Ar /H_2
Main gas [Ar]	≈ 46 SLPM 1.3 bar
Secondary gas [$\mathbf{H_2}$]	≈ 8.1 SLPM 1.5 bar
Current	600 A 64 V
Spray distance	150 mm

After coating the specimens by the prepared mixtures using the APS technique, the samples were subjected to metallurgical, morphological, mechanical (micro-hardness), and surface texture (Porosity and roughness) investigation.

Standard procedures of specimen preparation for metallographic examination were employed according to the following sequence; the metallographic cross-section samples for coating structure evaluation were cut from the coated specimens using a wire cutting machine. Then, the specimens were mounted in conventional Bakelite hot mounting material and pre-ground on the water as a –lubricant. Silicon Carbide abrasive, grade “120” was used as abrasive media to remove about 0.5 mm of the material. Standard grinding and polishing operations were carefully applied for metallographic observations.

The phase composition of composite coating was determined using an X-ray Diffractometer (XRD) (PANanalytical, X’Pert PRO) having Kα radiation with generator settings of 30 kV and 40 mA. Diffraction data were collected over a 2θ range of 5° - 100°, with a step width of 0.02°. The morphologies of as-sprayed coatings were examined using a Secondary Electron Microscope model FEI (Inspect S 50-Netherlands) with Energy Dispersive X-Ray Spectroscopy EDS attachment (Bruker AXS-Flash Detector 410-M, Germany). The microhardness of the as-sprayed coating was measured on polished surfaces using a standard (HV-1000) micro-hardness tester at a load of 300 g and a dwell period of 10 s. For each specimen, hardness tests were repeated ten times and the average value was recorded. The porosity percentage in the coatings was measured by using ImageJ analyzer software applying the

thresholding procedure. Surface roughness was measured using (TR 110) tester with five readings for each sample at least while recording the average values.

3. Result and Discussion

3.1 *Powder microstructural analysis*

Figure 2a, b shows the SEM micrographs of the mixtures of Ni/Al (80/20) and Ni5Al (95/5) with pure Aluminum, respectively. All powders have uneven morphologies, elongated straight, twisted, or spheroidal shapes, and irregular particle sizes. The particle size of pure Aluminum powder is 22 to 84 µm, while particle size of as-received Nickel-based powders Ni/Al (80/20) and Ni5Al (95/5) are 45 to 88 µm, and 50 to 110 µm, respectively. This diversity of Aluminum particle size affects directly the composition of coating and the formation of intermetallic compounds [7].

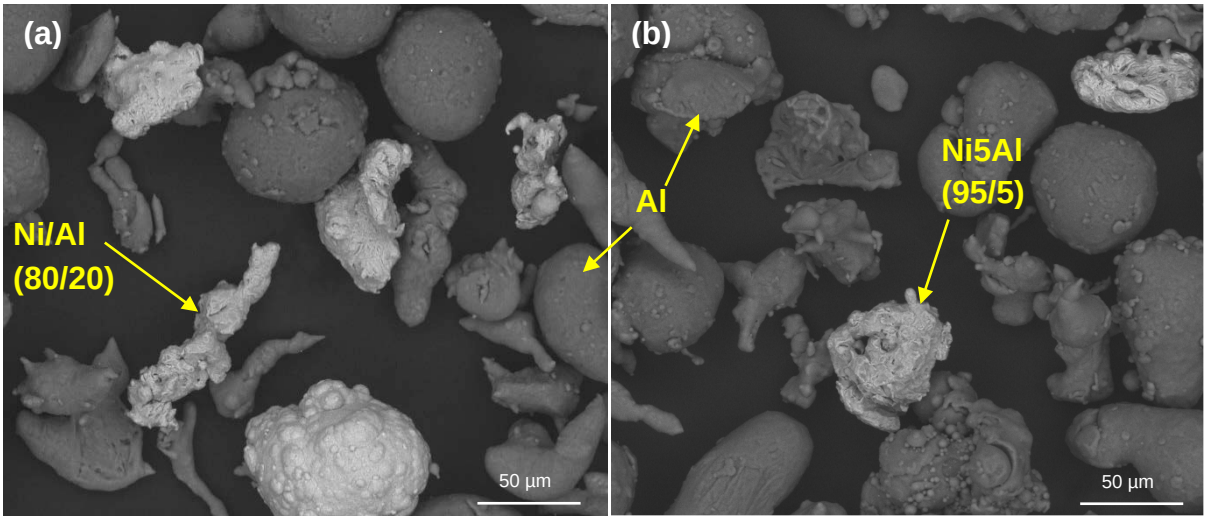

Figure 1SEM micrographs of (Metco™54-NS-1) Al powders with (a) Metco™404-NS, (b) Metco™450-NS

3.2 *XRD analysis of coatings*

Surveying previous studies have highlighted some important points to be considered before coating analysis. According to [7], the particle size of alumni affects directly the composition of coatings. NiAl formation is preferred with the aluminum size distribution 75 -100 m, whereas Ni3Al formation is preferred with small particles in the mixtures. Hussain in [37] stated that the ordered phases NiAl and Ni3Al appear at 50 and 75 atomic percent of Ni respectively based on the equilibrium phases diagram of Al-Ni.

Figure 3. shows the X-Ray Diffraction patterns of the coatings as deposited on stainless steel substrates. By comparing all the previously stated studies with the XRD analysis shown in Figure 2, two intermetallic compounds NiAl and Ni3Al appeared (most common phases in the phase equilibrium diagram of Ni-Al). The predominant phase was NiAl β-phase [23], which is found in all samples, even in the samples with the lowest Ni percentage (samples: 1A and 1B), despite the above-mentioned fact that states NiAl formation in the range of atomic percentage of Ni which is 50, ssssssssssssin aligning with the same research criteria of applying Ni5Al and Ni/Al powders by APS, the XRD patterns of Rizaee et al. [20] and Q. Jia et al. [45], respectively, revealed the formation of NiAl. Nevertheless, [20], [45] have stated the absence of Ni3Al ϒ-phase, which appears in samples 5A and 5B only. In these particular samples, the Ni-based powders are reached 50% of the coating.

Pure Al and Ni appeared in all patterns, whereas Al could be considered the coating matrix, while the intensities of Ni increased directly with the increment of Ni-based alloys in the mixture. XRD patterns shown in Fig. 2.a. indicate the absence of Al2O3 for samples with Ni-5Alpowders as indicated by Rizaee [20] in his research of Ni5Al by APS, whereas samples with Ni-Al powder in Fig. 2.b. shows the same result of Al2O3 absence, except in sample 5A at 2θ~66.8°, similar results were also illustrated by Kubatik research [17] with Ni10Al and Ni40Al by APS. It has been observed that NiO appears with the increase of the Ni-based percentage in samples 3B, 5A, and 5B. This mixture of metal and metal oxide could be harder than the metal coating itself but to a certain limit as stated in [2], [32].

3.3 Cross-sectional characterization of coatings

Figure 3 shows cross-sectional microstructures of all samples that exhibit some typical APS features similar to other studies [17], [31], [32], [46]. The coatings contain lamellar or layered splat structures (as a consequence of molten particles' impact on the substrate), entrapped unmelted particles, micro-pores, and oxides inclusions. Abu-Warda et al. [10], developed an Al2O3-30(Ni20Al) layer on 304 stainless steel with High-Velocity-Oxy-Fuel (HVOF) technique; the coating morphology was characterized by an irregular surface with quite similar morphology to our deposited layers with APS technique.

Aluminum can be considered as the coating matrix for all samples, the existence of lamellar light gray splats can be overseen. It increased gradually by increasing the content of the Ni-based compositions that reached its highest percentage in samples (5A and 5B). Oxides (Al2O3 and NiO) are generally seen as dark, elongated phases that appear as strings in the coating cross-section, parallel to the substrate. Neither micro-cracks nor large pores exist in all samples. No evidence of micro-cracks to be observed, but almost all samples show a small number of micro-pores. Generally, increasing the percentage of Nickel-based alloys enhances the uniformity of coating. Coatings of samples 1B, 3B, and 5B, Ni-based alloys were denser and bulkier, while they tended to be thinner and more flattened. All deposited APS layers had an average thickness of 350 ± 19 μm.

3.4 *Physical and mechanical properties of coatings*

Porosity and surface roughness of coating are connected, and both could be affected by different parameters, characteristics of powder, coating compositions, spraying distance, gun, or even substrate temperature [7]. Figure 4 shows that, with 15 cm spraying distance and different compositions of Ni-Al with pure Al, all samples had a normal range of porosity [47], although sample 5A has the maximum porosity percentage (7.443 %), It is still within the normal range from 40 to <1% [2]. Other literature has stated a similar porosity range. Javadi et al. [25] stated that the optimum spray distance for Ni-Al powders is 11 cm which resulted in 4.5% porosity of coating volume, Wang et al. [40] reported a low porosity percentage resulted for NiAl10. Nonetheless, Kubatík et al. [17] produced more porous phases of NiAl10 and NiAl40 with 22 % and 17 %, respectively.

Moreover, Figure 4 displays surface roughness which was approximately 6.242 ± 0.689 μm for all samples, where they are quite similar to the commercial alloy coatings [7].

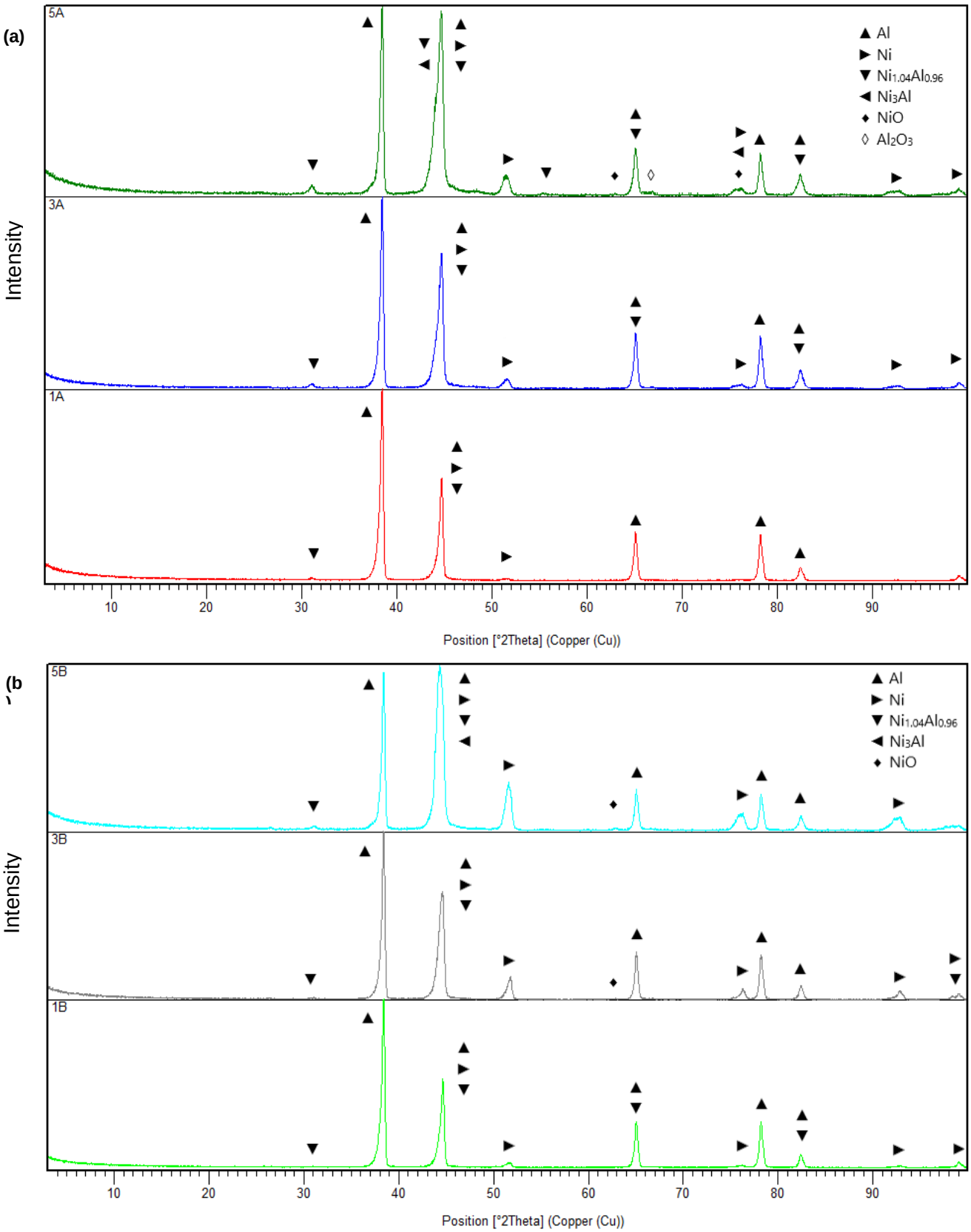

Figure 2 XRD patterns for coatings, (a) 1A, 3A, 5A; (b) 1B, 3B, 5B

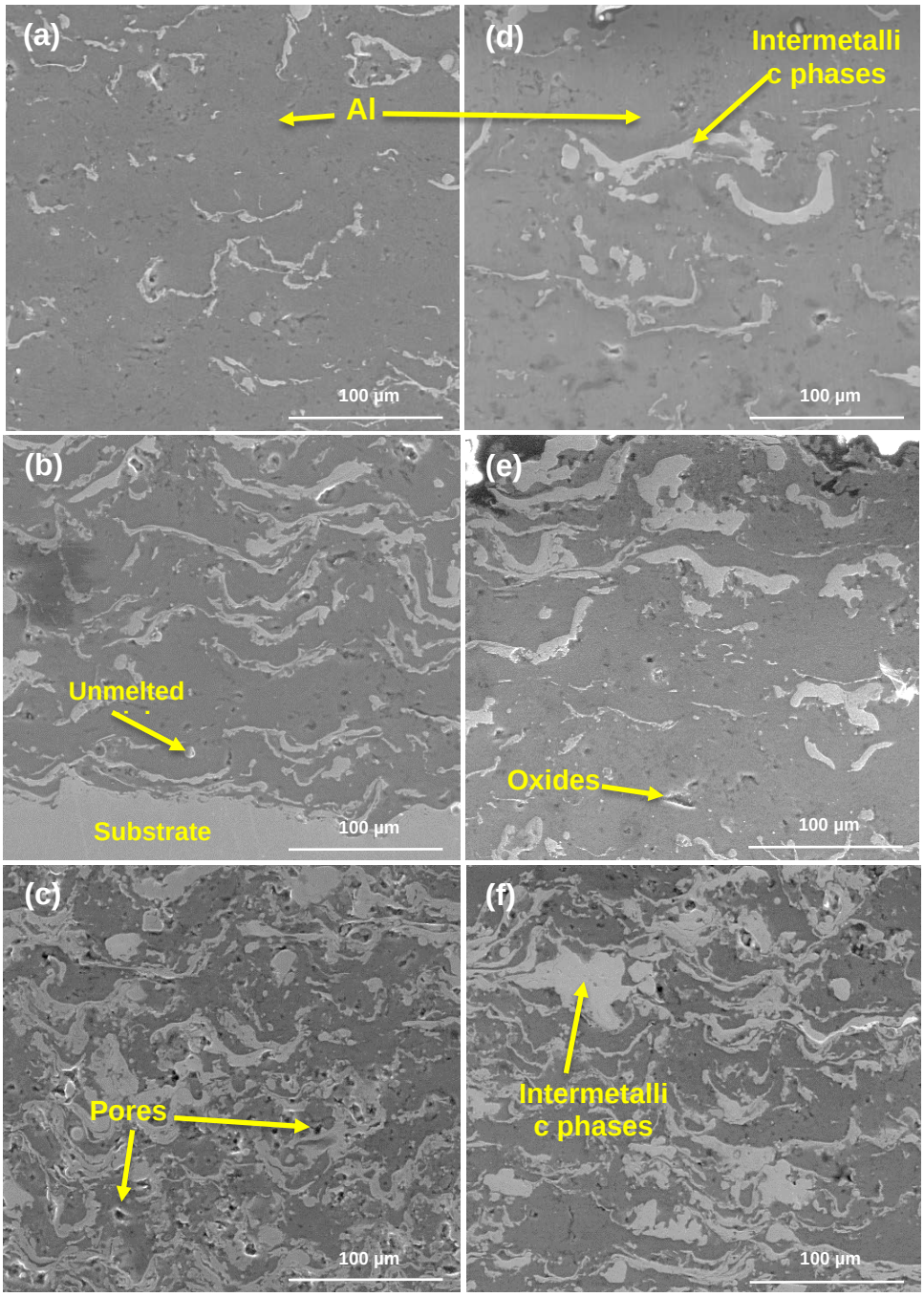

Figure 3 SEM micrographs of as-sprayed samples; (a) 1A, (b) 3A, (c) 5A, (d) 1B, (e) 3B and (f) 5B

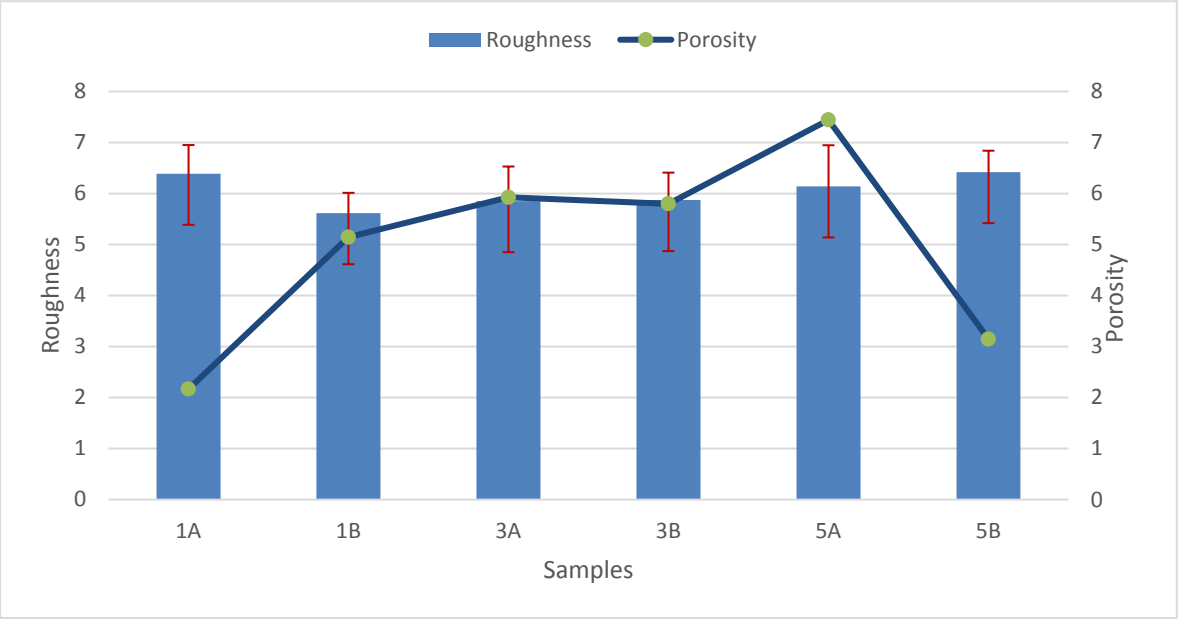

Figure 4 Coating properties; Porosity and Surface Roughness

Figure 5,a shows micrograph of microstructure of APS coating and substrate with indenter indentation. The cross-sectional zone of the substrate near the deposited layer has a noticeable color change, it could be attributed to the heat developed through the APS process which affects directly the physical characteristics. Moreover, microhardness values of the substrate in this interdiffusion zone (50 µm alongside coating) increase from 125 to 163 ± 8 HV as shown in Table 3, which is considered as proof positive for good interaction between substrate and coatings layers. Microhardness measurements of all samples are listed in Table 3 Both values of substrate and coating layers are included in Figure 5,b.Despite the increment in microhardness of this zone of interdiffusion, all samples exhibit different behavior, which is affected directly by the percentage of nickel [48]. Microhardness values of samples 1A and 1B are slightly higher than commercially pure Aluminum coating [49]. Therefore, the microhardness of both mixtures with the amount of Ni-based alloys below 30% is not a recommended type of as-sprayed coating for an application that requires adequate mechanical performance. By increasing the amount of Nickel-based alloys above 30 %, microhardness values reached an average of 164.5 HV with a standard deviation of 10.31 HV [21], [50]. It could be observed that the microhardness of the six different coatings was enhanced obviously by increasing the amount of Ni-based alloys in mixtures above 30%.

Table 3 Microhardness measurements of coatings and substrate

Sample No.	Interdiffusion Area (Substrate)	Coating layer
1A	155	74
1B	165	81
3A	158	149
3B	163	165
5A	167	167
5B	170	178

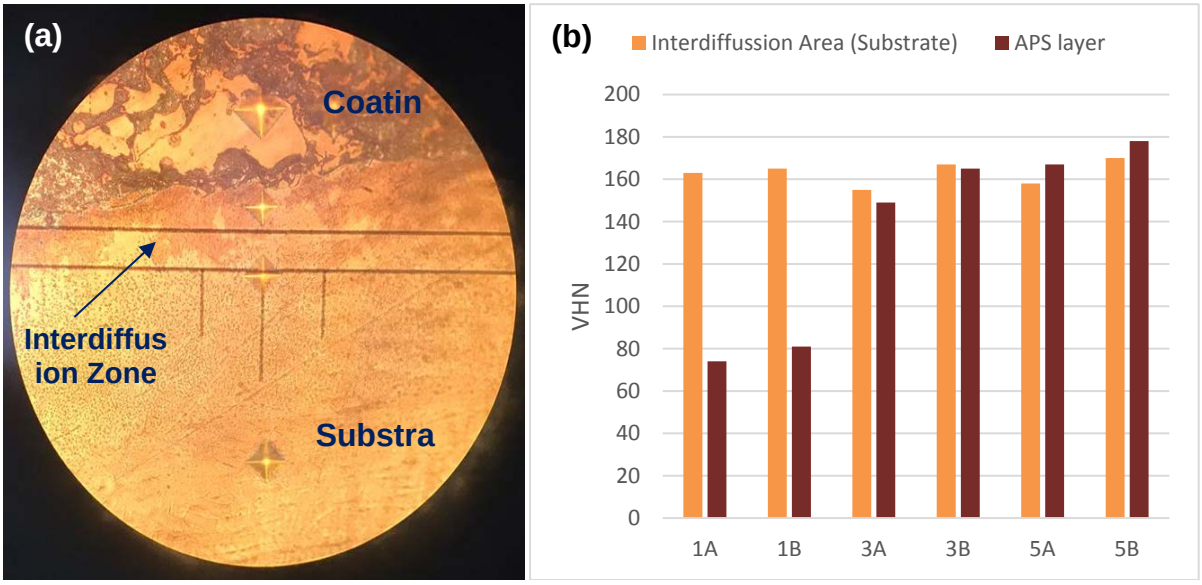

Figure 5(a) Details of the microstructures of both APS layer and substrate with indenter imprint after measurement. (b) Microhardness values for substrate's interdiffusion area and APS layers.

4. Conclusion:

This work has investigated the coating of stainless steel 304 by APS using Al, Ni/Al, and Ni5Al. Several observations were recorded as follows: Deposition of Aluminum powder separately mixed with Ni-Al and Ni 5Al results in a dense coat with no cracks or other major defects. The sample of Ni/Al and pure Al(5A) with 50% each has resulted in the highest porosity percentage which is still in the normal range stated in previous literature. Microhardness of the substrate (interdiffusion zone, 50 µm alongside coating) extensively increase compared to the average value of 304 SST microhardness. This is due to heat developed in the APS process. The measured microhardness of proposed coatings is affected directly by the percentage of Ni-based alloys in mixtures. Sample with Ni-based alloys in mixtures less than 30% have shown poor results. Formation of intermetallic compounds such as NiAl is inevitable in all samples, despite the amount of Ni-based alloys in mixtures, or even the atomic percentage of Ni; besides the existence of Ni3Al depends only on increasing the percentage of the Ni-based alloy to 50 % percent in the mixtures.

References

[1] Fauchais, P.L., Heberlein, J.V.R. and Boulos, M.I. (2014). Thermal Spray Fundamentals. Boston, MA: Springer US.
[2] Tucker, R.C. ed., (2013). Thermal Spray Technology. ASM International.
[3] Sampath, S., Jiang, X.Y., Matejicek, J., Prchlik, L., Kulkarni, A. and Vaidya, A. (2004). Role of thermal spray processing method on the microstructure, residual stress and properties of coatings: an integrated study for Ni–5 wt.%Al bond coats. Materials Science and Engineering: A, **364(1-2)**, pp.216–231.
[4] Guo, R.Q., Zhang, C., Yang, Y., Peng, Y. and Liu, L. (2012). Corrosion and wear resistance of a Fe-based amorphous coating in underground environment. Intermetallics, **30**, pp.94–99.
[5] Gupta, M., Markocsan, N., Li, X.-H. and Peng, R.L. (2017). Improving the lifetime of suspension plasma sprayed thermal barrier coatings. Surface and Coatings Technology, **332**, pp.550–559.
[6] Wang, Y., Yang, Y. and Yan, M.F. (2007). Microstructures, hardness and erosion behavior of thermal sprayed and heat treated NiAl coatings with different ceria. Wear, **263(1-6)**, pp.371–

378.
[7] Xanthopoulou, G., Marinou, A., Vekinis, G., Lekatou, A. and Vardavoulias, M. (2014). Ni-Al and NiO-Al Composite Coatings by Combustion-Assisted Flame Spraying. Coatings, **4(2)**, pp.231–252.
[8] Lukauskaitė, R., Černašėjus, O., Škamat, J., Zabulionis, D., Stonys, R., Kalpokaitė-Dičkuvienė, R. and Antonovič, V. (2017). The effect of Al Mg substrate preparation on the adhesion strength of plasma sprayed Ni Al coatings. Surface and Coatings Technology, **316**, pp.93–103.
[9] Ang, A.S.M. and Berndt, C.C. (2014). A review of testing methods for thermal spray coatings. International Materials Reviews, **59(4)**, pp.179–223.
[10] Abu-warda, N., López, A.J., López, M.D. and Utrilla, M.V. (2019). High temperature corrosion and wear behavior of HVOF-sprayed coating of Al2O3-NiAl on AISI 304 stainless steel. Surface and Coatings Technology, **359**, pp.35–46.
[11] Sun, C., Hui, R., Qu, W. and Yick, S. (2009). Progress in corrosion resistant materials for supercritical water reactors. Corrosion Science, **51(11)**, pp.2508–2523.
[12] Li, Y., Wang, S., Sun, P., Xu, D., Ren, M., Guo, Y. and Lin, G. (2017). Early oxidation mechanism of austenitic stainless steel TP347H in supercritical water. Corrosion Science, **128**, pp.241–252.
[13] Rodriguez, D. and Chidambaram, D. (2015). Oxidation of stainless steel 316 and Nitronic 50 in supercritical and ultrasupercritical water. Applied Surface Science, **347**, pp.10–16.
[14] Subramanian, C. (2010). Wear properties of aluminium-based alloys. Surface Engineering of Light Alloys, pp.40–57.
[15] Khandanjou, Sh., Ghoranneviss, M. and Saviz, Sh. (2017). The detailed analysis of the spray time effects of the aluminium coating using self-generated atmospheric plasma spray system on the microstructure and corrosion behaviour. Results in Physics, **7**, pp.1440–1445.
[16] Kadir, NF., Manap, A., Satgunam, M. and Afandi, N.M. (2018). Review on Nickel Aluminide based Bond Coat Properties and Oxidation Performance for Thermal Barrier Coating (TBC) Application. International Journal of Engineering & Technology, **7(4.35)**, p.624.
[17] Kubatík, T.F., Lukáč, F., Stoulil, J., Ctibor, P., Průša, F. and Stehlíková, K. (2017). Preparation and properties of plasma sprayed NiAl10 and NiAl40 coatings on AZ91 substrate. Surface and Coatings Technology, **319**, pp.145–154.
[18] Orban, R.L., Lucaci, M., Rosso, M. and Grande, M.A. (2007). NiAl Oxidation and Corrosion Resistant Coatings Obtained by Thermal Spraying. Advanced Materials Research, **23**, pp.273–276.
[19] Properties and Selection: Nonferrous Alloys and Special-Purpose Materials. (1990). Asm International.
[20] Rezaee Hajideh, M., Farahani, M., Pakravan, M. and Shahmirzalo, A. (2019). Corrosion resistance and hydrophilic properties of plasma sprayed Ni+5%Al coatings. Heliyon, **5(6)**, p.e01920.
[21] Wang, X., Feng, X., Lu, C., Yi, G., Jia, J. and Li, H. (2018). Mechanical and tribological properties of plasma sprayed NiAl composite coatings with addition of nanostructured TiO2/Bi2O3. Surface and Coatings Technology, **349**, pp.157–165.
[22] Tao, X.P., Zhang, S., Zhang, C.H., Wu, C.L., Chen, J. and Abdullah, A.O. (2018). Effect of Fe and Ni contents on microstructure and wear resistance of aluminum bronze coatings on 316 stainless steel by laser cladding. Surface and Coatings Technology, **342**, pp.76–84.
[23] Fan, X., Zhu, L. and Huang, W. (2017). Investigation of NiAl intermetallic compound as bond coat for thermal barrier coatings on Mg alloy. Journal of Alloys and Compounds, **729**, pp.617–626.
[24] Han, Y., Yang, K., Jing, P., Xue, B. and Ma, W. (2018). Mechanical and tribological properties of NiAl/muscovite composites. Journal of Alloys and Compounds, **741**, pp.765–774.
[25] Javadi, M.M., Edris, H. and Salehi, M. (2011). Plasma Sprayed NiAl Intermetallic Coating Produced with Mechanically Alloyed Powder. Journal of Materials Science & Technology,

27(9), pp.816–820.
[26] Bochenek, K. and Basista, M. (2015). Advances in processing of NiAl intermetallic alloys and composites for high temperature aerospace applications. Progress in Aerospace Sciences, **79**, pp.136–146.
[27] Li, B., Gao, Y., Han, M., Guo, H., Jia, J., Wang, W. and Deng, H. (2017). Tribological properties of NiAl matrix composite coatings synthesized by plasma spraying method. Journal of Materials Research, **32(9)**, pp.1674–1681.
[28] Wu, Q., Li, S., Ma, Y. and Gong, S. (2013). Study on behavior of NiAl coating with different Ni/Al ratios. Vacuum, **93**, pp.37–44.
[29] Li, B., Jia, J., Gao, Y., Han, M. and Wang, W. (2017). Microstructural and tribological characterization of NiAl matrix self-lubricating composite coatings by atmospheric plasma spraying. Tribology International, **109**, pp.563–570.
[30] Poliarus, O., Morgiel, J., Umanskyi, O., Pomorska, M., Bobrowski, P., Szczerba, M.J. and Kostenko, O. (2019). Microstructure and wear of thermal sprayed composite NiAl-based coatings. Archives of Civil and Mechanical Engineering, **19(4)**, pp.1095–1103.
[31] Fan, X., Huang, W., Zhou, X. and Zou, B. (2020). Preparation and characterization of NiAl–TiC–TiB2 intermetallic matrix composite coatings by atmospheric plasma spraying of SHS powders. Ceramics International, **46(8)**, pp.10512–10520.
[32] Shi, P., Wan, S., Yi, G., Sun, H., Yu, Y., Xie, E., Wang, Q., Shen, S.Z. and Alam, N. (2020). TiO2–ZnO/Ni–5wt.%Al composite coatings on GH4169 superalloys by atmospheric plasma spray techniques and theirs elevated-temperature tribological behavior. Ceramics International, **46(9)**, pp.13527–13538.
[33] Mahesh, R.A., Jayaganthan, R. and Prakash, S. (2008). A study on hot corrosion behaviour of Ni–5Al coatings on Ni- and Fe-based superalloys in an aggressive environment at 900°C. Journal of Alloys and Compounds, **460(1-2**), pp.220–231.
[34] La, P., Bai, M., Xue, Q. and Liu, W. (1999). A study of Ni3Al coating on carbon steel surface via the SHS casting route. Surface and Coatings Technology, **113(1-2)**, pp.44–51.
[35] Marinou, A., Xanthopoulou, G., Vekinis, G., Lekatou, A. and Vardavoulias, M. (2015). Synthesis and heat treatment of sprayed high-temperature NiAl–Ni3Al coatings by in-flight combustion synthesis (CAFSY). International Journal of Self-Propagating High-Temperature Synthesis, **24(4)**, pp.192–202.
[36] Mishra, S.B., Chandra, K., Prakash, S. and Venkataraman, B. (2005). Characterisation and erosion behaviour of a plasma sprayed Ni3Al coating on a Fe-based superalloy. Materials Letters, **59(28)**, pp.3694–3698.
[37] A. Hussain, M. A. Choudhry, and S. S. Hayat. (2009). Effects of ordering on the thermal properties of an Ni3Al intermetallic alloy system: A molecular dynamics approach. Chinese J. Phys., **vol. 47, no. 3**, pp. 344–354.
[38] M. I. K, S. S. Havaldar, and A. Hiriyannaiah. (2021). Materials Today : Proceedings Composition optimization for NiAl + Al 2 O 3 + CeO composite coating on bearing steel by air plasma spray. Mater. Today Proc, pp. 2–7.
[39] Bhosale, D.G. and Rathod, W.S. (2020). Investigation on wear behaviour of SS 316L, atmospheric plasma and high velocity oxy-fuel sprayed WC-Cr3C2-Ni coatings for fracturing tools. Surface and Coatings Technology, **390**, p.125679.
[40] Wang, C., Gao, P., Liu, T., Li, L., Wang, E. and Wang, Q. (2019). Microstructure and wear performance of Ni-10 wt.%Al coatings plasma sprayed on Ni-based superalloys with a sound field. Surface and Coatings Technology, **370**, pp.157–162.
[41] Esmaeili, Z., Loghman-Estarki, M.R., Ramezani, M., Naderi, M. and Mohammad Sharifi, E. (2020). Toward hardening of NiCrAlY alloy by spark plasma sintering of NiCrAlY-nanoSi3N4-graphite nanocomposite. Journal of Alloys and Compounds, **847**, p.155802.
[42] Ma, Y., Li, W., Guo, M., Yang, Y., Cui, Y., Sun, W., Dong, Y. and Yan, D. (2021). TiC-TiSi2-Al2O3 composite coatings prepared by spray drying, heat treatment and plasma

spraying. Journal of Alloys and Compounds, **857,** p.158221.
[43] Beyhaghi, M., Kiani-Rashid, A.-R., Kashefi, M., Khaki, J.V. and Jonsson, S. (2015). Effect of powder reactivity on fabrication and properties of NiAl/Al2O3 composite coated on cast iron using spark plasma sintering. Applied Surface Science, **344**, pp.1–8.
[44] Yu, Y., Zhou, J., Ren, S., Wang, L., Xin, B. and Cao, S. (2016). Tribological properties of laser cladding NiAl intermetallic compound coatings at elevated temperatures. Tribology International, **104**, pp.321–327.
[45] Jia, Q., Li, D., Li, S., Zhang, Z. and Zhang, N. (2018). High-Temperature Oxidation Resistance of NiAl Intermetallic Formed In Situ by Thermal Spraying. Coatings, **8(8)**, p.292.
[46] Rukhande, S.W. and Rathod, W.S. (2020). An isothermal oxidation behaviour of atmospheric plasma and high-velocity oxy-fuel sprayed nickel-based coating. Ceramics International, **46(11)**, pp.18498–18506.
[47] Pawlowski, L. (2008). The Science and Engineering of Thermal Spray Coatings.
[48] Yamanoglu, R., Karakulak, E., Zeren, M. and Koç, F.G. (2013). Effect of nickel on microstructure and wear behaviour of pure aluminium against steel and alumina counterfaces. International Journal of Cast Metals Research, **26(5)**, pp.289–295.
[49] Kubatík, T.F., Ctibor, P., Mušálek, R. and Janata, M. (2017). Mechanical properties of plasma-sprayed layers of aluminium and aluminium alloy on AZ 91. Materiali in tehnologije, **51(2)**, pp.323–327.
[50] Gautam, R.K.S., Rao, U.S. and Tyagi, R. (2019). High temperature tribological properties of Ni-based self-lubricating coatings deposited by atmospheric plasma spray. Surface and Coatings Technology, **372**, pp.390–398.